Hydraulic efficiency and optimization of pipe culvert inlet edges

By Joakim Sellevold, Oddbjørn Bruland and Elena Pummer

Joakim Sellevold (M.Sc) is a senior engineer at Statens vegvesen, and a Ph.D-candidate at NTNU.
Oddbjørn Bruland (Ph.D) is a professor at NTNU.
Elena Pummer (Ph.D) is an associate professor at NTNU.

Sammendrag

Hydraulisk effektivitet for innløpskanter i sylindriske rørkulverter. Rørkulverter er mye brukt for drenering og flomsikring av veier i Norge. Denne artikkelen beskriver sammenhengene mellom kantuformingen og den hydrauliske effektiviteten til kulvertinnløp under forskjellige strømningsforhold. Resultatene viser at nødvendig geometri for økt eller optimal hydraulisk effektivitet kan bestemmes for et bredt spenn av utforminger, definert ut fra innløpstype og kantgeometri. Denne geometrien er beskrevet for rett-, muffe-, skrå- og avrundede kanter for innløp med frontmur og utstikkende innløp. Resultatene indikerer at en kantgeometri som følger en elliptisk bue kan sikre høy hydraulisk effektivitet under både innløp- og utløpskontroll. Usikkerheten i datagrunnlaget er ukjent, og videre arbeid er derfor nødvendig for å validere egenskapene til denne kanttypen. Videre arbeid er også nødvendig for å komplettere eksisterende data og bestemme optimal utforming for tilskårede innløp. De generelle sammenhengene mellom kantutforming og hydraulisk effektivitet åpner for utvikling av mer effektive prefabrikkerte innløp.

Summary

Pipe culverts are widely used for drainage and flood protection of roads in Norway. This paper reviews the effects of culvert inlet edges geometry on hydraulic efficiency. It was found that the necessary edge geometry could be determined for a wide range of designs, defined by inlet type and edge geometry. The required edge sizes are included for square, socket, bevel and rounded edges, for headwall and projecting inlets. The results indicate that an elliptical arc edge geometry can ensure high hydraulic efficiency under both inlet and outlet control conditions. The uncertainty of the reviewed data and methods is not known, and further testing is therefore necessary to validate the properties of this edge design. Further testing is also necessary in order to complement existing data and to determine the optimum design for mitered inlets. The reported, generalized results allow for development of more efficient prefabricated inlets.

Notation

A = Culvert barrel cross section area [m^2]
A_η = Cross section area of control section [m^2]
c = Submerged discharge coefficient [s^2/ft]
C_D = Inlet discharge coefficient [-]
C_η = Control surface discharge coefficient [-]

D = Culvert rise/diameter [m]
D_η = Control section rise/diameter [m]
g = Gravitational acceleration (9.81) [m/s^2]
H_w' = Effective total head [m]
H^* = Dimensionless head [-]
k = Slope correction coefficient [-]
k_D = Inlet pressure term [-]
k_e = Entrance loss coefficient [-]
k_η = Control section pressure term [-]
K = Unsubmerged discharge coefficient [-]
K_u = Unit conversion factor (1.811) [ft$^{0.5}$/m$^{0.5}$]
l = Inlet projection length [m]
M = Unsubmerged discharge exponent [-]
Q = Discharge [m^3/s]
Q^* = Semi-dimensionless discharge [ft$^{0.5}$/s]
R^2 = Coefficient of determination [-]
t = Inlet wall thickness [m]
v = Average flow velocity [m/s]
Y = Pressure term [-]
ΔH_e = Entrance head loss [m]
Δr = Edge width (radial direction) [m]
Δl = Edge length (longitudinal direction) [m]
Δt = Additional edge width (radial direction) [m]
α = Circle segment central angle [rad]
η = Orientation of the control surface tangent [°]
θ = Bevel edge orientation [°]

Introduction

Use and design of road culverts in Norway

More than 550.000 culverts are used for cross drainage and flood protection of roads in Norway. Due to increased recognition of flood risk and climate change, the required design discharge for road culverts in Norway has increased significantly over the last 50 years (Statens vegvesen, 1977; 1992; 2011; 2018; 2022) (fig. 1a). A significant number of existing culverts is therefore assumed to be under designed with regards to hydraulic capacity (Statens vegvesen, 2021) (fig. 1b). For this reason, there is a general need for cost effective and hydraulically efficient inlets for both new construction and replacement of existing culverts. Hydraulic design methods for culverts are generally based on the results of physical scale model experiments and cover a wide range of culvert inlet designs and flow conditions (French, 1955; Schiller, 1956; French, 1961; McEnroe and Johnson, 1995; Smith and Oaks, 1995; Graziano et al. 2001, Schall et al. 2012). The Federal Highway Administration (FHWA) framework (Schall et al. 2012) uses a special case design methodology, where the entrance loss coefficient for outlet control (OC) and semi-dimensionless head-discharge relationships for inlet control (IC) are given, valid for specific combinations of inlet type, cross section shape, and inlet edge geometry.

Hydraulic efficiency of culverts

The hydraulic efficiency of a culvert inlet can be defined as its ability to effectively utilize available head to transport water (Schall et al. 2012). High hydraulic efficiency results in lower relative headwater elevations for a given discharge and can therefore reduce the risks of cross

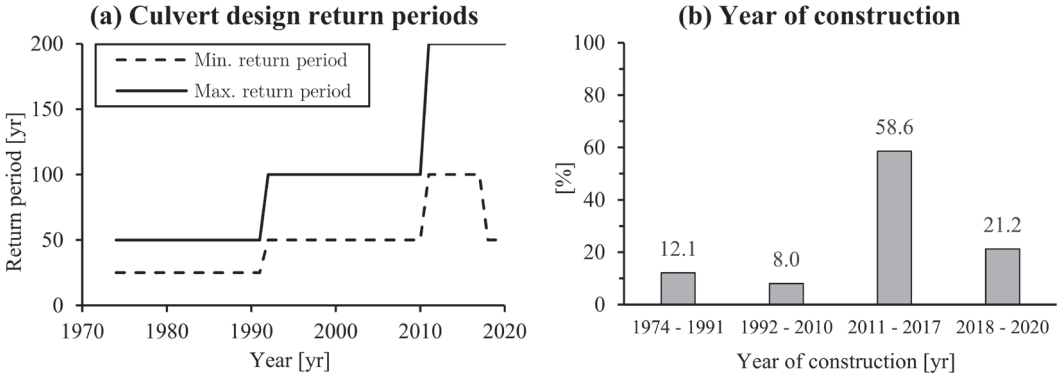

Fig. 1. Design return periods and year of construction for Norwegian road culverts (1974 - 2020).

drainage failure, local flooding, rerouting of water, and also reduce the effects of inlet blockage (Weeks et al. 2009; Schall et al. 2012). Highly efficient inlet designs include side- and slope tapered inlets and Minimum Energy Loss (MEL) culverts (Schall et al. 2012). However, approximately 90% of the roughly 550.000 road culverts in Norway are commercially available, premanufactured, cylindrical pipe culverts, and the registered data shows no use of these inlet or culvert types (Gianni et al. 2022). Significant increases in efficiency can, however, also be obtained using favorable inlet edge geometries (French, 1961; Idelchik, 1986; Schall et al. 2012). The present FHWA design framework covers a limited number of efficient inlet edge geometries for bevel, socket and rounded edges.

Research objectives

Due to the tradition of using premanufactured, cylindrical pipe culverts in the Norwegian road sector, this study was limited to reviewing the effects of the inlet edge geometry on the hydraulic efficiency of cylindrical pipe culverts. Cylindrical pipe culvert inlets are defined by inlet type (headwall, projecting or mitered) and edge type (square, bevel, socket or rounded). The first objective of this study was to determine the inlet edge geometry required for hydraulic improvement and optimization for all combinations of inlet and edge type. The second objective was to evaluate the potential for further development of compact, efficient inlet edge geometries, based on the available design methods and data. The present study was limited to evaluation of hydraulic efficiency in terms of entrance loss coefficients and head-discharge relationships, consistent with the present FHWA framework for hydraulic culvert design (Schall et al. 2012).

Culvert hydraulics

Under OC conditions, the energy loss associated with the inlet is given by the entrance loss coefficient (k_e) and the velocity head (Schall et al. 2012):

$$\Delta H_e = k_e \frac{v^2}{2g} \tag{1}$$

The k_e values are valid for submerged outlet control (pressure) flow where the width of the approach channel is large compared to the diameter of the pipe culvert (Idelchik, 1986). OC efficiency is here defined by k_e, with a low value indicating high efficiency.

Under IC conditions, Schall et al. (2012) gives the relationships between dimensionless head ($H^* = H_w'/D$) and semi-dimensionless discharge ($Q^* = K_u Q/AD^{0.5}$). The design equations use empirical design parameters (K, M, c and Y) valid for specific inlet designs:

Unsubmerged: $$\frac{H_w}{D} = K\left(\frac{K_u Q}{AD^{0.5}}\right)^M \tag{2}$$

Submerged: $$\frac{H_w'}{D} = c\left(\frac{K_u Q}{AD^{0.5}}\right)^2 + Y \tag{3}$$

IC efficiency is here defined by the H^*/Q^* ratio, with a smaller ratio indicating higher efficiency. While eq. 2 and 3 can be used to show trends of hydraulic efficiency based on the inlet edge geometry, they cannot be used to determine the required geometry for ensuring a specified efficiency. Eq. 2 and 3 were adapted from the experimental results of French (1955; 1961) for cylindrical culverts, where it is reported that the IC efficiency of inlets is governed mainly by the location and orientation of the control surface that impinges on the flowing water, relative to the barrel axis (η):

Unsubmerged:

$$\frac{H_w'}{D} = \frac{D_\eta}{D}\frac{k\,(C_\eta)^{0.5}}{2}\left(\frac{1}{k\,(C_\eta)^{2.5}\left(\frac{A_\eta}{A}\right)^2\left(\frac{D_\eta}{D}\right)}\right)^{0.304}\left(\frac{K_u Q}{AD^{0.5}}\right)^{0.607} \tag{4}$$

Submerged: $$\frac{H_w'}{D} = \frac{1}{2g\left(C_\eta\frac{A_\eta}{A}\right)^2}\left(\frac{K_u Q}{AD^{0.5}}\right)^2 + k_\eta \tag{5}$$

Eq. 4 was found by regression of the results of French (1961), and approximates the mean H^*-Q^* relationship for a wide range of inlets. Some differences between eq. 2 and 4 are therefore to be expected. French (1961) also deter-

mined the general flow control condition under IC conditions:

$$C_D = \min\left(C_\eta \frac{A_\eta}{A}\right) \quad (6)$$

In physical terms, eq. 6 states that the section of the inlet that yields the highest value of H^* will limit flow and define the discharge coefficient for the inlet (C_D). French (1961) determined that optimal performance is achieved when the limiting section is located at the transition between the inlet edge and the barrel (throat section, subscript t). Design values for eq. 4 – 6 for bevel and rounded edges are given in table 1 and 2. The uncertainty of eq. 4 and 5 and the data in tables 1 and 2 is not known (French, 1961).

Inlet edge geometry

The different pipe culvert inlet and edge types are shown in fig. 2. In order to determine the edge geometry based on required hydraulic performance, the relative edge width ($\Delta r/D$), length ($\Delta l/D$) and pipe thickness (t/D) must be defined as a function of the cross-section area of the throat (A) and the cross section area of an arbitrary upstream control section (A_η). For flush invert inlets and exposed invert edges, the area ratio (A_η/A) relationship can be found as follows (fig. 2f):

Table 1. Design values for bevel edge control surfaces - eq. 4 - 6 (data from French, 1961).

η	10°	20°	30°	40°	50°	60°	70°	80°	90°	180°
C_η	0.921	0.872	0.822	0.772	0.723	0.682	0.656	0.636	0.624	0.510
k_η	0.930	0.880	0.840	0.790	0.750	0.710	0.690	0.670	0.660	0.590

Table 2. Design values for rounded edges - eq. 4 - 6 (data from French, 1961).

r_e/D	0.000	0.040	0.080	0.100	0.125[a]	0.250
C_D	0.624	0.712	0.763	0.786	0.821	0.899
k_D	0.660	0.740	0.780	0.780	0.830	0.970

[a]Interpolated using eq. 14 and 15 (table 8 in the Appendix).

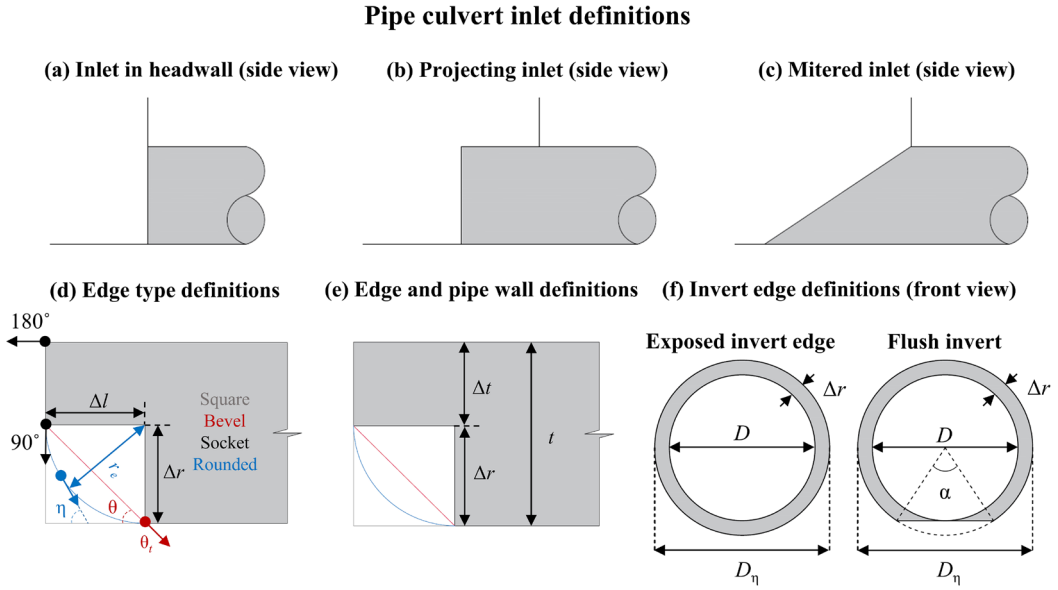

Fig. 2. Cylindrical inlet type and edge geometry definitions.

Flush invert:

$$\frac{A_\eta}{A} = \left(1 + \frac{2\Delta r}{D}\right)^2 - \frac{\left(1 + \frac{2\Delta r}{D}\right)^2 (\alpha - \sin\alpha)}{2\pi} \quad (7)$$

Exposed invert edge:

$$\frac{A_\eta}{A} = \left(1 + \frac{2\Delta r}{D}\right)^2 \quad (8)$$

For bevel edges, the relative edge length ($\Delta l/D$) can be found using the relationship $\Delta l/D = (\Delta r/D \times 1/\tan\theta)$. For rounded edges of constant edge radius, $r_e/D = \Delta r/D = \Delta l/D$ applies (fig. 2d). For inlets in a headwall, $\Delta t/D$ is large compared to $\Delta r/D$, and the least efficient applicable control surface is $\eta = 90^\circ$ (fig. 2d). For projecting inlets of wall thickness t, $t = \Delta r + \Delta t$ applies, and the least efficient applicable control surface is $\eta = 180^\circ$ (fig. 2d and e).

Edge geometry optimization (IC)

To determine the inlet geometry required for IC throat control, eq. 4 and 6 were used to determine the necessary A_η/A ratios for unsubmerged and submerged conditions, respectively. Because eq. 4 estimates a mean H^*-Q^*-relationship, eq. 6 was used to determine necessary edge widths, and the unsubmerged condition was included only for comparison. Eq. 7 and 8 were used to determine the corresponding values of $\Delta r/D$ for flush and exposed invert edges, respectively. Eq. 4 and 5 were then used to determine the H^*-Q^* relationships for each edge type. French (1961) reported significant variation in the pressure term (k_η) with the discharge coefficient (C_η). It was therefore conservatively assumed $k_\eta = k_t =$ constant, and that the radial location of the control edge relative to the throat does not significantly influence C_η for cross sections upstream from the throat section. The effects of $\Delta l/D$ on effective head (H_w') and friction losses were also neglected, under the assumption that $\Delta l/D$ is small. A culvert slope of 0.03 m/m was chosen, corresponding to $k = 0.92$ in eq. 4 (French, 1961). Note that the edge sizes given in this section are minimum required edge sizes, and that larger edge sizes will yield similar hydraulic performance under IC conditions. Edge sizes smaller than those given in this section will not ensure throat control, but will improve the efficiency to some degree. For both cases, the hydraulic performance can be estimated using eq. 4 and 5. Finally, it was assumed that flush inverts and exposed invert edges only affect the cross-section area ratio (A_η/A) and not the hydraulic efficiency, as flow separation has been found to be suppressed near the invert of the inlet (French, 1961).

Square, bevel and socket edges (IC)

The design values in table 1 were used to determine the required edge geometry for square, bevel and socket edges, for both headwall and projecting inlets. In fig. 3, the necessary edge widths for square ($\theta = 90^\circ$) and bevel ($10^\circ < \theta < 90^\circ$) edges are shown for both flush and exposed invert edges. The hydraulic performance for $10^\circ < \theta < 90^\circ$ is given in fig. 4. The difference between the two curves for $\theta = 90^\circ$ in fig. 3b shows that optimum efficiency for a square edge projecting inlet is achieved when $\Delta t/D + \Delta r/D \geq 0.05$. French (1961) found that socket edges behaved similarly to bevel edges, where the two edge corners define θ relative to the barrel axis (fig. 2d). However, this conclusion was based on a limited number of experimental results (French, 1961). To the degree that socket and bevel edges have identical hydraulic properties, fig. 3 covers all potential square, bevel and socket edge geometries for $10^\circ < \theta < 90^\circ$. Comparison to side tapered inlets from French (1961) and Schall et al. (2012) in fig. 3b shows that for $\theta < 30^\circ$, the design values of table 1 leads to an underestimation of $\Delta r/D$ for $\eta = 90^\circ$ (headwall) and overestimation for $\eta = 180^\circ$ (projecting). In this regard, it should be noted that French (1961) only tested bevel edges of $\theta \geq 30^\circ$, and that for $\theta < 30^\circ$, the design values for bevel edges in table 1 are extrapolated (French, 1961). Regression analysis of the results showed that the required values of $\Delta r/D$ and $\Delta t/D$ could be accurately estimated as a function of the bevel angle (θ) (table 7 in the Appendix).

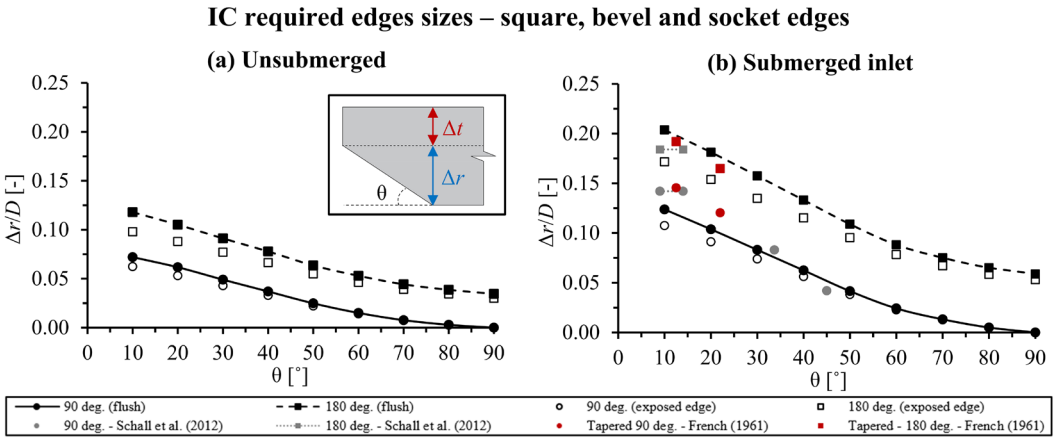

Fig. 3. Required edge width for 0° ≤ θ ≤ 90° (data from French, 1961 and Schall et al. 2012).

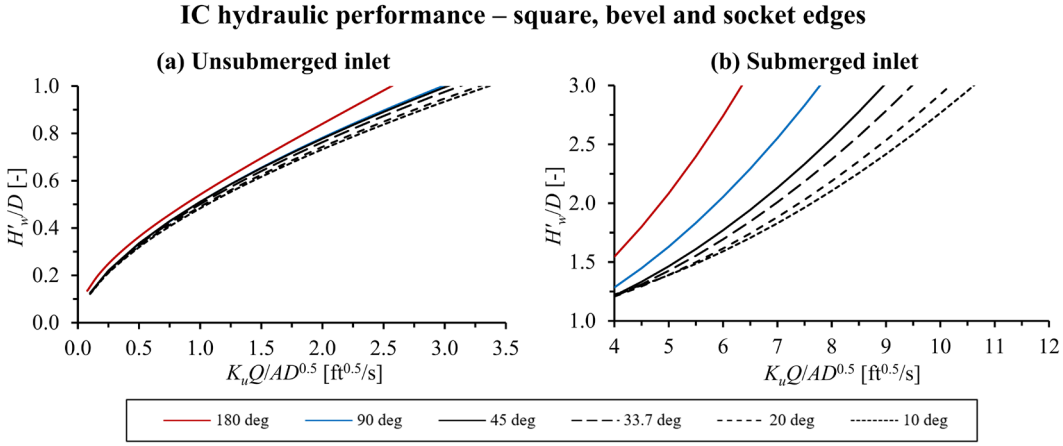

Fig. 4. H-Q* relationships for square, bevel and socket edged inlets (data from French, 1961).*

Rounded edges (IC)

The design values in table 2 were used to determine the required edge geometry for rounded edges, for both headwall and projecting inlets. To use these values with eq. 4 and 5, $A_\eta/A = 1.0$, $C_D = C_\eta$ and $k_D = k_\eta$ were used. French (1961) found that for rounded edges, the control section would intersect the curved surface, placing it upstream of the throat. Fig. 5 shows the necessary geometries for rounded edges. For submerged IC conditions (fig. 5b), projecting inlets require an additional edge width (Δt) for $r_e/D \leq 0.155$ for flush invert inlets and $r_e/D \leq 0.125$ for exposed invert inlets. The corresponding H^*-Q^* relationships are plotted in fig. 6, with the η = 90° and 10° conditions from fig. 4 for reference. Fig. 6 shows that while efficiency increases with r_e/D, the performance is still within that of η = 90° and 10° for bevel edges, consistent with a control surface located on the curved edge surface (French, 1961). The difference in required edge size between flush and exposed invert inlets was found to be significant for rounded edges (fig. 5b). Regression analysis showed that C_D, k_D and values of $\Delta r/D$ and $\Delta t/D$ could be estimated as a function of r_e/D (table 8 in the Appendix).

Mitered inlets (IC)

Mitered inlets are associated with low IC efficiency (French, 1955; Schall et al. 2012), but can be improved using a favourable inlet edge

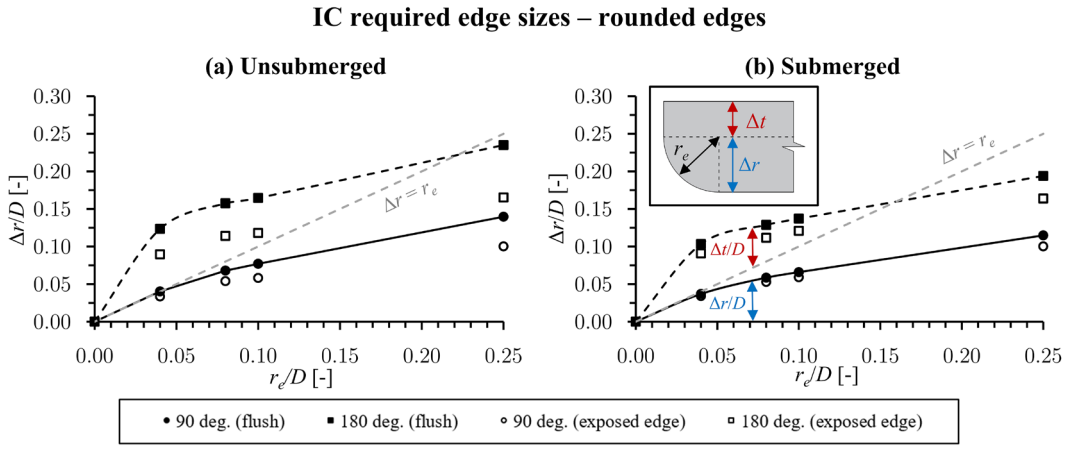

Fig. 5. Necessary edge geometry for rounded edges (data from French, 1961).

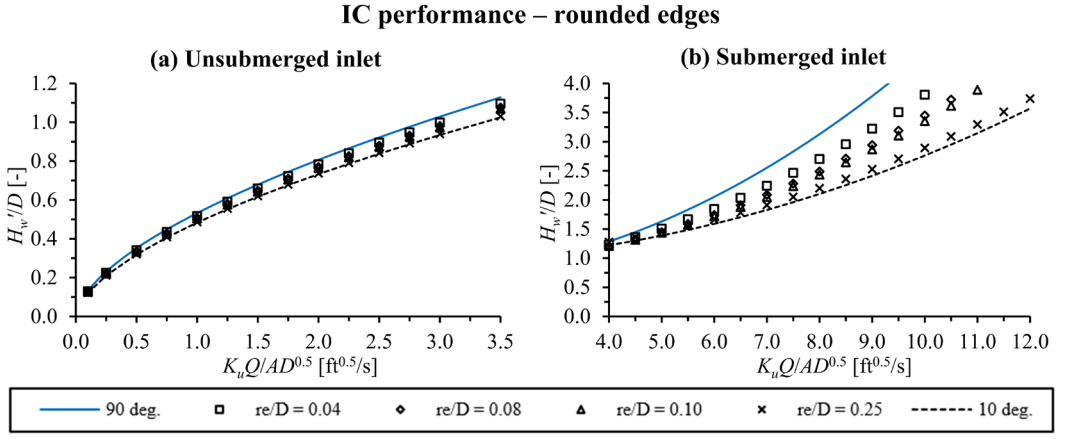

Fig. 6. H-Q* relationships for rounded edges (data from French, 1961).*

(Schiller, 1956) or flared (tapered) end sections (French, 1961; McEnroe & Johnson, 1995; Smith and Oaks, 1996; Graziano et al. 2001). The reader is referred to the referenced publications for detailed descriptions of the inlet designs. The referenced publications used equations and dimensionless groups different from those of Schall et al. (2012), and regression analysis was therefore used to determine the design parameters for eq. 2 and 3 (table 3). It should be noted that of the referenced studies for mitered inlets, only French (1961) used vented inlets to reduce sub-atmospheric air pressure in the culvert barrel. The values of *c* and *Y* in table 3 are therefore associated with uncertainty, as sub-atmospheric pressure in the barrel is known to increase submerged hydraulic efficiency at small scales (French, 1961). Graziano et al. (2001) reported measurements of H_w'/D only up to 1.2 – 1.4, and found large variations in submerged efficiency between experiments, and these results were therefore not included in the comparison. The *H*-Q** relationships are plotted in fig. 7, with the η = 90° and η = 10° conditions from fig. 4 for reference. The comparison in fig. 7 shows clearly that while rounded inlet edges and flared end sections improve efficiency, mitered inlets generally yield lower efficiency than headwall inlets of similar edge treatment. It was found that there was insufficient data to determine the hydraulic efficiency as a function of the inlet design parameters.

Table 3. Regression values for eq. 2 and 3 (data from referenced publications).

Reference	Inlet description	*K*	*M*	*c*	*Y*
French (1955)	Mitered (1:2)	0.528	0.588	0.0463	0.75
Schiller (1956)	Mitered ($r_e/D = 0.125$)	0.555	0.505	0.0316	0.694
McEnroe & Johnson (1995)	Flared end section – concrete	0.527	0.537	0.0336	0.575
	Flared end section – steel	0.500	0.588	0.0390	0.648
Smith & Oak (1995)	Armtec	0.561	0.555	0.0373	0.730
	Modified Armtec	0.539	0.565	0.0279	0.794

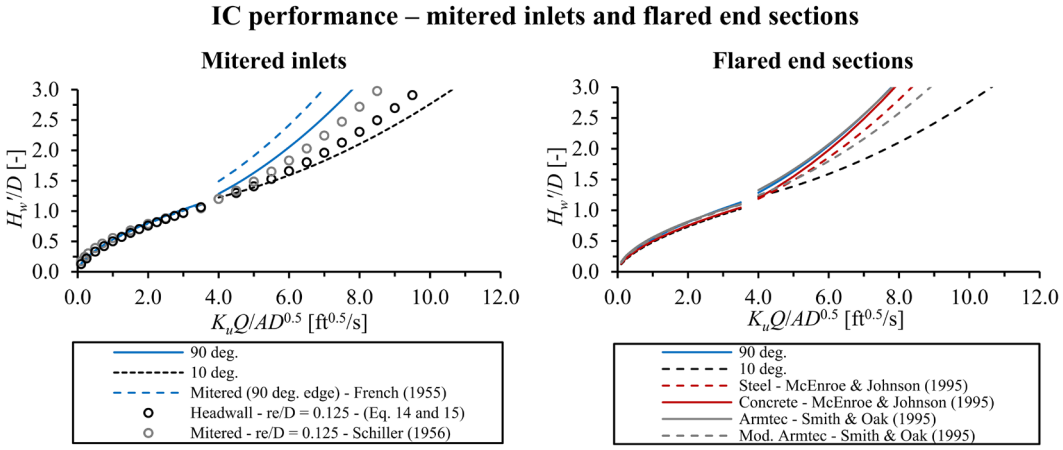

Fig. 7. Mitered inlets and flared end sections, compared to 90 and 10 deg. control conditions.

Edge geometry optimization (OC)

To determine OC efficiency, k_e values for the different inlet and edge types were evaluated. The entrance loss coefficients are valid for exposed invert edge inlets under pressure flow conditions and the uncertainty of k_e is not known.

Square edges (OC)

For square edged inlets, k_e is a function of the relative projection length (l/D) and the relative wall thickness (t/D) (Idelchik, 1986). The dependencies are shown in fig. 8, and indicate that for projecting inlets, significant increases in efficiency can be obtained through the use of increased pipe thickness, flange or similar design, such that $t/D \geq 0.05$, similarly to the results for IC conditions.

Bevel edges (OC)

For bevel edges, k_e depends on the bevel angle and size (Idelchik, 1986). Idelchik (1986) notes that for bevel edges, flow separation and energy losses occur both at the face and throat sections, and that the sum of these are minimized for $\theta \approx 20^\circ - 30^\circ$, yielding the lowest values of k_e (fig. 9 and 10). Using the relative bevel widths ($\Delta r/D$) from fig. 3 for optimized IC efficiency, the k_e values in table 4 were determined from fig. 9 and 10. The results show that k_e is low, but higher than those of socket or rounded edges for similar edge widths. However, since IC performance is influenced mainly by the orientation of the control surface, edge sizes can be increased for improved OC performance without significantly changing IC performance. For small values of θ, $\Delta l/D$ is large, and friction losses could potentially reduce efficiency under both IC and OC

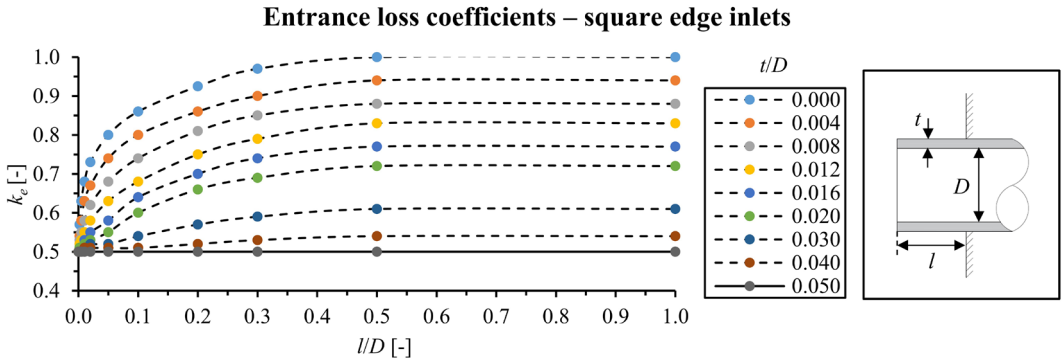

Fig. 8. Entrance loss coefficients for square edged inlets (data from Idelchik, 1986).

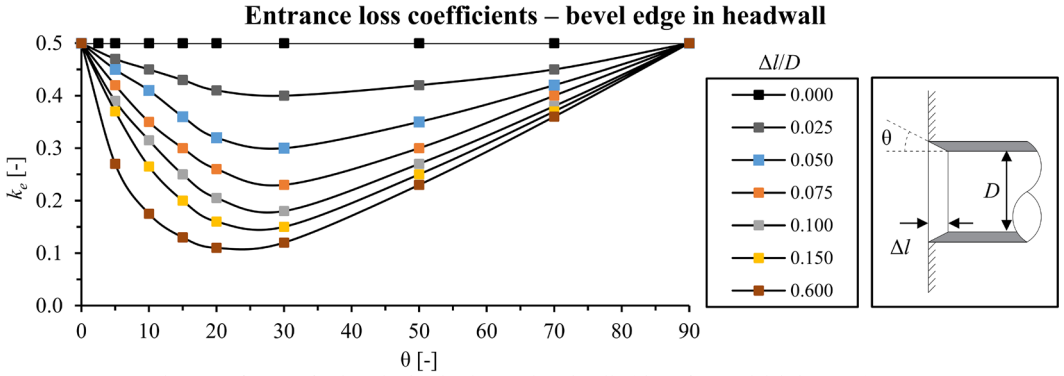

Fig. 9. Entrance loss coefficients for bevel edged inlets in headwalls (data from Idelchik, 1986).

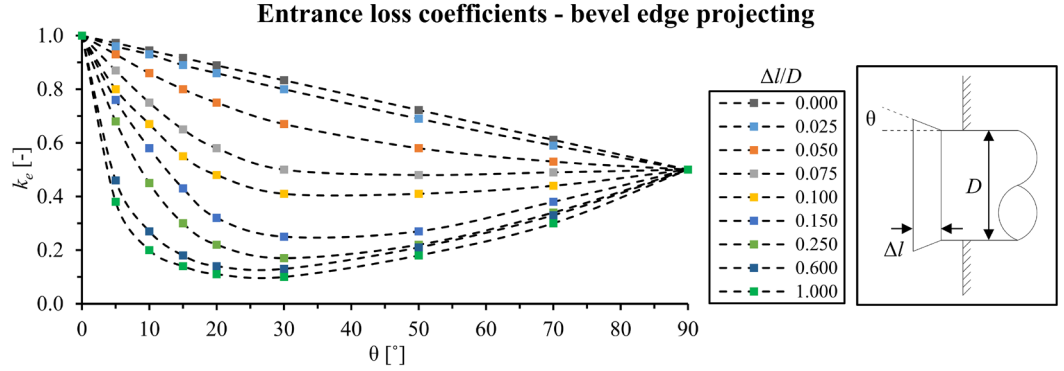

Fig. 10. Entrance loss coefficients for projecting beveled inlet (data from Idelchik, 1986).

conditions (French, 1961; Idelchik, 1986). It should also be noted that for θ = 45˚, Idelchik (1986) gives k_e = 0.34 (headwall) and 0.40 (projecting), which is higher than k_e = 0.2, given in Schall et al. (2012).

Socket edges (OC)

For socket edges, Idelchik (1986) describes only the optimized edge design for socket edges (table 5). From this limited data, it is not possible to make a general comparison to other edge types, but it should be noted that the optimized socket edges yield both lower k_e values and

Table 4. Entrance loss coefficients for inlets optimized for IC conditions (fig. 3) (data from Idelchik, 1986).

θ [°]	Headwall inlets			Projecting inlets		
	Δr/D [-]	Δl/D [-]	k_e [-]	Δr/D [-]	Δl/D [-]	k_e [-]
10.0	0.124	0.703	0.16	0.172	0.975	0.20
20.0	0.104	0.286	0.15	0.154	0.423	0.20
33.7	0.070	0.105	0.19	0.128	0.192	0.20
45.0	0.050	0.050	0.34	0.105	0.105	0.40

Table 5. Entrance loss coefficients for socket edge inlets (data from referenced publications).

Reference	Inlet	Δr/D [-]	Δl/D [-]	θ [°]	k_e [-]
Schall et al. (2012)	Socket edge (headwall or projecting)	0.05	0.07	39.5	0.2
Idelchik (1986)	Socket edge (headwall)	0.15	0.20	36.9	0.10 - 0.12
Idelchik (1986)	Socket edge (thin-walled projecting)	0.10	0.25	21.8	0.10 - 0.12

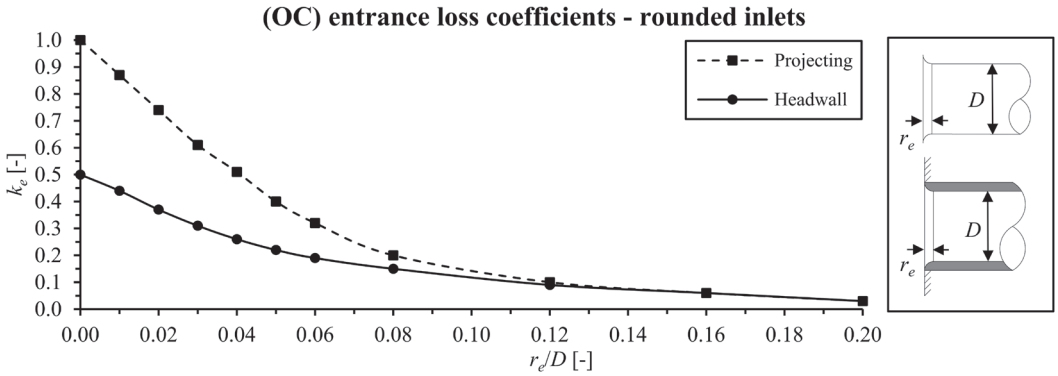

Fig. 11. Entrance loss coefficients for rounded inlet edges (data from Idelchik, 1986).

shorter required edge lengths ($\Delta l/D$) than bevel edges of similar bevel angles (fig. 9 and 10).

Rounded edges (OC)

Rounded edges are known to yield high OC efficiency (Idelchik, 1986). Fig. 11 shows k_e as a function of r_e/D and shows values of $k_e \leq 0.1$ are obtained for $r_e/D \geq 0.125$, giving lower values than for bevel edges of similar width. This differs from the performance of rounded edges under IC conditions, where rounded edges limit the hydraulic efficiency compared to optimized bevel edges. It should also be noted that the difference in k_e between headwall and projecting inlets is negligible for $r_e/D > 0.125$, similarly to IC conditions for exposed invert edges (fig. 5b).

Mitered inlets (OC)

Entrance loss coefficients for different mitered inlets and flared (tapered) end sections are given in table 6. The reader is referred to the referenced publications for detailed descriptions of the inlet designs. The results shows that flared end sections yield higher efficiency than straight mitered inlets, but that efficiency decreases with the length of the flared section ($\Delta l/D$). Comparison to fig. 8 - 11 shows that for similar values of ($\Delta l/D$), the mitered inlets yield significantly lower OC efficiency than bevel edge inlets in

Table 6. Entrance loss coefficients for mitered inlets (data from referenced publications).

Reference	Inlet	θ [°]	Δl/D [-]	k_e [-]
Schall et al. (2012)	Straight mitered (1:2)	0.0	0.00	0.7
Smith & Oak (1995)	Straight mitered (1:2)	0.0	0.00	1.06
McEnroe & Johnson (1995)	Flared end section - concrete	16.0	1.60 - 2.00	0.31
	Flared end section - steel	17.0	1.45 - 1.70	0.24
Smith & Oak (1995)	Flared - Armtec	18.0	1.75	0.60
	Flared - Mod. armtec	18.0	1.75	0.42
Graziano et al. (2001)	Iowa DOT prefabricated inlet	8.0 – 11.0	1.42 - 2.00	0.31 - 0.38

headwalls. The results of Smith and Oak (1995) deviate significantly from the other studies, and it should be noted that for the "Armtec" design, the culvert barrel projects a small distance upstream into the flared end section. According to the data presented in table 6, flared end sections improve hydraulic efficiency compared to straight mitered inlets, but there is insufficient data to determine k_e as a function of the inlet design parameters.

Potential for improved edge geometry for IC and OC conditions

The results show that bevel, socket and rounded edges of significant size can be used to ensure high efficiency under IC and OC conditions. For bevel edges of small values of θ, flow separation is significant around the upstream edge (Idelchik, 1986). For small values of θ, rounding of the upstream edge could therefore potentially reduce k_e. An edge of this type is similar in principle to a tapered inlet with a favorable face edge geometry (Schall et al. 2012). This design could potentially reduce the required edge length, while ensuring throat control for a range of throat bevel angles (θ_t). The necessary edge geometry for this edge type was calculated using eq. 6 and 7, and the design values in table 1. The results are the required A_η/A and $\Delta r/D$ values for an inlet edge with a constant C_D value (table 9 in the Appendix). Fig. 12 shows C_D as a function of the relative horizontal location of the cross section ($x/\Delta l$) and edge geometries for θ_t = 10°, 20° and 33.7°. These θ_t values were chosen to cover the span of throat angles between bevel edges ($\theta \geq 33.7°$) and side tapered inlets ($9.5° \leq \theta \leq 14°$) in the present FHWA design framework. For comparison, bevel and rounded edges of similar efficiency are included, taken from fig. 3 (bevel edges) and eq. 16 (rounded edges). The vertical, continuous lines in fig. 12 show required additional edge width ($\Delta t/D$). As can be seen in fig. 12a, c and e, both bevel and rounded edges result in C_D > min. (C_D) for parts of the inlet edge. It should be noted that the C_D values for the rounded edges in fig. 12 were calculated using the design values of table 1, and that the resulting C_D values are up to 5.1 % higher than for the bevel edges. This indicates a hydraulic difference between rounded and beveled edges and is consistent with the findings of French (1961) for rounded edges.

Discussion

Generalized v. special case framework

The reviewed data and methods show that the hydraulic efficiency of a wide range of pipe culvert inlets can be determined based on the inlet edge geometry for both IC and OC conditions. Due to the lower estimation accuracy of eq. 4, eq. 6 was used to estimate the necessary edge sizes. Since the edge geometries, k_e and the H^*-Q^* relationships are given in (semi-) dimensionless form, the results are valid for a wide range of culvert sizes (French, 1961; Idelchik; 1986; Schall et al. 2012). As IC efficiency is mainly influenced by the control section orientation (η) and cross section area (A_η/A), it is possible to

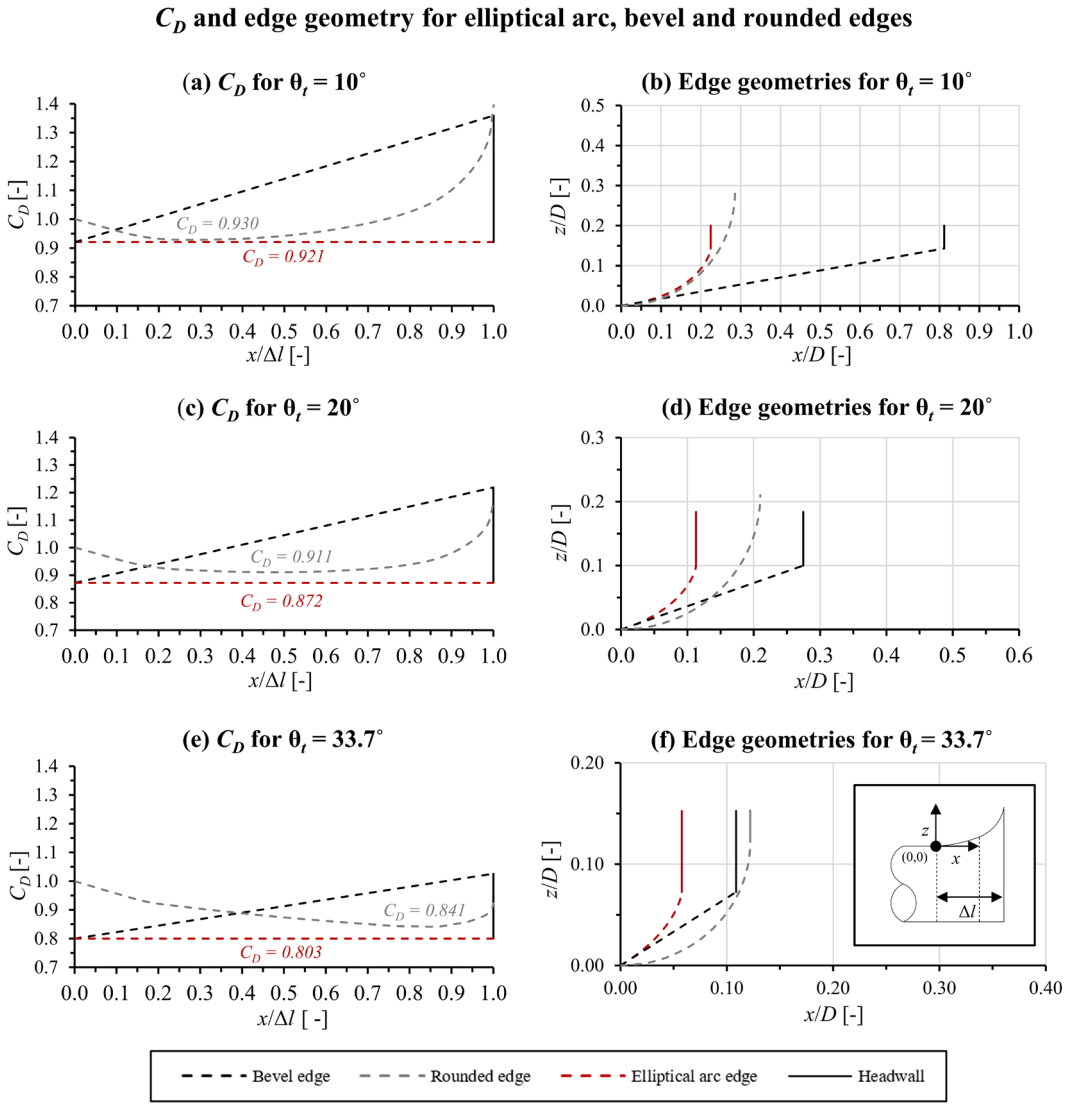

Fig. 12. Non-linear edge geometry (data from French, 1961).

increase the edge size beyond that required to ensure IC throat control to increase OC efficiency. However, the effects of friction losses and effective head should be considered for longer edges (French, 1961; Idelchik, 1986). The results show that while different edge geometries can yield high hydraulic efficiency under both IC and OC conditions, there are notable differences that make it challenging to fully optimize a single edge geometry for both flow conditions.

The regression analysis showed that the necessary edge geometry could generally be accurately estimated using polynomial equations, allowing for easy and precise implementation of the results (table 7 and 8 in the Appendix). Due to the differences in required edge width for bevel edges (table 1) and side-tapered inlets in fig. 3, eq. 10 is recommended for determining the required bevel edge width ($\Delta r/D$) for bevel edges of $\theta < 30°$. For rounded edges, French

(1961) found differences up to 3.4 % between experimental C_D values and C_D values estimated using the data of table 1. Eq. 14 – 20 are therefore recommended for determining the required hydraulic properties and required edge geometry for rounded edges. For the rounded edges, the relationship between the pressure term (k_D) and the relative edge radius (r_e/D) showed the lowest coefficient of determination (R^2 = 0.983). This is in general agreement with the results of French (1961), who reported significant variation in the pressure term (k_D). Further work covering potential difference between socket and bevel edges, bevel edges of $\theta < 30$, and rounded edges of $0.10 < r_e/D < 0.25$ is warranted, in order to complement existing data.

The special case framework of Schall et al. (2012) is widely used, and differences between assumed and actual, as-built inlet edge geometries is a source of uncertainty in hydraulic design. The results obtained in this paper reduces this uncertainty, but since both the experimental uncertainty and the uncertainty associated with eq. 4 and 5 are not known, a direct comparison of these uncertainties is not possible.

Elliptical arc edge geometry

The elliptical arc edge geometry was derived using eq. 6 and 7 and the design values from table 1, with the goal of determining a compact edge geometry that results in a constant C_D value for a specified throat angle under IC conditions. Due to the differences between the results obtained using the design values in table 1 and both side-tapered inlets (fig. 3) and rounded edges (fig. 12), further work is recommended to validate the IC efficiency of the elliptical arc edge geometry. For OC conditions, Idelchik (1986) states that the lowest loss coefficients are found for "*smooth inlets, the cross section of which forms an arc of a circle, etc.*". Entrance loss coefficients of k_e = 0.03 – 0.06 have also been found for elliptical arc inlet edges for reservoir outlets (Liskovec, 1951). Since the edge geometries of fig. 12 resemble elliptical arcs, they can be expected to yield high OC efficiency. However, further work is required to validate the specific C_D and k_e values, or to further develop the edge geometries of fig. 12.

Further work

Physical model testing and/or computational fluid dynamic (CFD) simulations are required to complement the existing data and verify the estimated hydraulic efficiency of the elliptical arc inlet edges. To conform to the minimum performance methodology of Schall et al. (2012), further study should account for subatmospheric air pressure in the culvert barrel under submerged IC conditions. Uncertainty of the hydraulic data and design parameters should also be evaluated, as the uncertainty of the reviewed experimental results is unknown.

Practical application

Hydraulic efficiency can, in general, reduce the risks of cross drainage failure, through the reduction of headwater elevation for a given discharge. This is seen clearly in the significant differences in submerged IC performance in fig. 4b, 6b and 7, and low k_e values of certain inlet edge designs. In addition, the increase in headwater elevation (IC) and k_e (OC) due to blockage, will generally be lower for efficient inlets (Weeks et al. 2009). Since there is significant uncertainty associated with estimated design flood discharges and in situ blockage of culvert inlets during floods, it is recommended that hydraulic efficiency should generally be as high as practically and economically possible, even for culverts designed for unsubmerged operation. The results presented in this paper allow for improvement or optimization of hydraulic efficiency of a wide range of pipe culvert inlets. However, culvert inlet design is not based on hydraulic efficiency alone, but also the cost and difficulty of production, construction, and maintenance (Schall et al. 2012). As such, the practical application of the results lies in the ability to optimize hydraulic efficiency based on a wide range of design constraints, such as pipe or headwall thickness, inlet edge length, and economic and practical constraints such as required material use, costs and carbon

footprint related to production, transport, and installation of the inlet. With regards to practical application, Schall et al. (2012) states that "... *while the use of curved surfaces rather than plane surfaces might result in slightly improved hydraulic efficiency at times, the advantages are outnumbered by the construction difficulties*". While this might generally be true in the context of in situ culvert construction, it is not necessarily the case for premanufactured inlets, using modern production methods and equipment. For these reasons, the most useful application of the results of this study lies in optimization of standardized edge designs for premanufactured pipe culverts. The generalized approach is based on the same experimental data as the special case FHWA framework (Schall et al. 2012), and complements the inlet designs presently included therein. For IC conditions, design values (K, M, c and Y) for improved or optimized inlets for use with eq. 2 and 3 can be determined through the use of eq. 4 and 5, allowing for direct implementation of the results.

Conclusion

Available culvert design methods and data have been reviewed to determine the required edge geometry and corresponding hydraulic properties for a wide range of pipe culvert inlet edge designs, under both IC and OC conditions. The results show that optimizing the inlet design for hydraulic efficiency results in different designs for IC and OC conditions:

- For square edged projecting inlets, maximum efficiency is achieved for both flow types by ensuring a wall thickness of $t/D \geq 0.05$ for both OC and IC conditions.
- For bevel edge inlets, the required edge size can be determined for IC conditions, and increased to improve OC efficiency, but friction losses should be evaluated for longer edges under both conditions. The results of Idelchik (1986) and design values of Schall et al. (2012) show significant differences for the 45° bevel in headwall inlet.
- For socket edged inlets, the behavior is similar to that of bevel edges for IC conditions. Under OC conditions, the necessary socket edge size is smaller than for bevel edges.
- For rounded edges, IC efficiency is lower than for bevel edges for similar edge widths. Under OC conditions, rounded edges yield the highest efficiency, and $k_e \leq 0.1$ can be achieved for $r_e/D \geq 0.125$.

The results are given in dimensionless form and cover a wide range of inlet edge designs. The most useful practical application of the results lies in improvement or optimization of premanufactured pipe culvert inlet edges, where the corresponding design values can be calculated for use with existing special case frameworks. The results of this study suggest that an edge geometry approximating an elliptical arc could optimize hydraulic efficiency for both IC and OC conditions, while minimizing the required edge size. These edges can be adapted to different throat angles and could be a valuable addition to the edge types presently included in the FHWA framework. However, due to the uncertainties associated with the design methods and data used, the elliptical arc geometry should be considered a basis for further study, using physical model experiments or CFD simulations. Further research is also required to determine potential differences more accurately between socket and bevel edges, the efficiency of bevel edges of $\theta < 30°$, efficiency of rounded edges of $0.10 < r_e/D < 0.25$ and the design values for improved mitered inlets, necessary for optimization of this inlet type.

Acknowledgements

This research was funded, in whole or in part, by The Research Council of Norway Project 312001. For the purpose of open access, the author has applied a CC BY 4.0 public copyright license to any Author Accepted Manuscript (AAM) version arising from this submission. The authors also want to thank Statens vegvesen for funding this study.

References

French J. L. (1955). *First progress report on hydraulics of short pipes – hydraulic characteristics of commonly used pipe entrances.* National Bureau of Standards, U.S. Department of Commerce.

French, J. L. (1961). *Fourth Progress Report On Hydraulics of Culverts – Hydraulics of Improved Inlet Structures for Pipe Culverts.* National Bureau of Standards, U.S. Department of Commerce.

Gianni, J., Nilsen, V., Sellevold, J., Molstad, L. (2022). *Assessment of culvert data from Bane NOR and the Norwegian Public Roads Administration.* Tidsskriftet VANN Vol. 2, 2022.

Graziano, F., Stein, S., Umbrell, E. & Martin, B. (2001). *Hydraulics of Iowa DOT Slope-Tapered Pipe Culverts.* U.S. Department of Transportation, Federal Highway Administration, Virginia.

Idelchik, I.E. (1986). *Handbook of hydraulic resistance.* Springer-Verlag, New York. 2nd edition.

Liskovec, L. (1951). *A study of the inlet shape of reservoir outlets.* Transactions, vol. 2 – Fourth Congress on Large Dams. New Delhi.

McEnroe, B.M. and Johnson, L.M. (1995). *Hydraulics of Flared End Sections for Pipe Culverts*. Transportation Research Board, Transportation Research Record 1483, Washington DC.

Schall, J.D., Thompson, P.L., Zerges, S.M., Kilgore, R.T. & Morris, J.L. (2012). *Hydraulic design of highway culverts.* Federal Highway Administration. U.S. Department of Transportation. 3rd edition.

Schiller Jr, R.E. (1956): *Tests on Circular-Pipe-Culvert Inlets.* Highway Research Board Bulletin 126. National Academy of Sciences. 13 p.

Smith, C.D. and Oak, A.G. (1995). *Culvert inlet efficiency.* Can. J. Civ. Eng. 22, 611 – 616.

Statens vegvesen (1977): *Håndbok 018 – Vegbygging.* Statens vegvesen, 1977.

Statens vegvesen (1992): *Håndbok 018 – Vegbygging.* Statens vegvesen, 1992.

Statens vegvesen (2011): *Håndbok 018 – Vegbygging.* Statens vegvesen, 2011.

Statens vegvesen (2018): *Håndbok N200 – Vegbygging.* Statens vegvesen, 2018.

Statens vegvesen (2021): *Nasjonal vegdatabank*. URL: https://vegkart.atlas.vegvesen.no/ (online, 02.12.2021).

Statens vegvesen (2022): *Vegnormal N200 – Vegbygging.* URL: https://store.vegnorm.vegvesen.no/n200_2022 (online, 15.06.2023).

Weeks, B. Barthelmess, A., Rigby, E., Witheridge, G. and Adamson, R. (2009). *Blockage of Hydraulic Structures. Stage 1 Report.* Engineers Australia, Barton ACT, Australia.

Appendix – Regression analysis results

The results of the regression analysis for bevel and rounded edges under submerged IC conditions are given in table 7 and 8.

Table 7. Regression results for square, bevel and socket edges – submerged IC.

Inlet type	Regression equation	Eq.
Headwall - table 1 (flush invert)	$\Delta r/D = -3.920 \times 10^{-8}\ \theta^3 + 1.871 \times 10^{-5}\ \theta^2 - 3.431 \times 10^{-3}\ \theta + 2.402 \times 10^{-1}$ | $(R^2 = 0.997)$	(9)
Headwall - maximum (flush invert)	$\Delta r/D = 8.528 \times 10^{-8}\ \theta^3 + 9.626 \times 10^{-6}\ \theta^2 - 3.682 \times 10^{-3}\ \theta + 1.920 \times 10^{-1}$ | $(R^2 = 0.998)$	(10)
Headwall (exposed invert)	$\Delta r/D = 1.664 \times 10^{-7}\ \theta^3 - 1.542 \times 10^{-5}\ \theta^2 - 1.311 \times 10^{-3}\ \theta + 1.222 \times 10^{-1}$ | $(R^2 = 1.000)$	(11)
Projecting (flush invert)	$\Delta r/D + \Delta t/D = 1.779 \times 10^{-7}\ \theta^3 - 1.425 \times 10^{-5}\ \theta^2 + 1.735 \times 10^{-3}\ \theta + 1.426 \times 10^{-1}$ | $(R^2 = 1.000)$	(12)
Projecting (exposed invert)	$\Delta r/D + \Delta t/D = 1.861 \times 10^{-7}\ \theta^3 - 1.746 \times 10^{-5}\ \theta^2 + 1.425 \times 10^{-3}\ \theta + 1.877 \times 10^{-1}$ | $(R^2 = 1.000)$	(13)

Table 8. Regression results for rounded edges – submerged IC.

Inlet type	Regression equation	Eq.
Discharge coefficient	$C_D = -3.853\ (r_e/D)^2 + 2.060\ (r_e/D) + 0.624 \mid (R^2 = 0.996)$	(14)
Pressure term	$k_D = -1.037\ (r_e/D)^2 + 1.492\ (r_e/D) + 0.660 \mid (R^2 = 0.983)$	(15)
Relative radius	$r_e/D = 2.494\ C_D^2 - 2.892\ C_D + 0.834 \mid (R^2 = 1.000)$	(16)
Headwall (flush invert)	$\Delta r/D = -8.167 \times 10^{-1}\ (r_e/D)^2 + 6.062 \times 10^{-1}\ (r_e/D) + 1.424 \times 10^{-2} \mid (R^2 = 0.999)$	(17)
Headwall (exposed invert)	$\Delta r/D = -7.385 \times 10^{-1}\ (r_e/D)^2 + 5.274 \times 10^{-1}\ (r_e/D) + 1.450 \times 10^{-2} \mid (R^2 = 0.992)$	(18)
Projecting (flush invert)	$\Delta r/D + \Delta t/D = -9.674 \times 10^{-1}\ (r_e/D)^2 + 7.106 \times 10^{-1}\ (r_e/D) + 7.672 \times 10^{-2} \mid (R^2 = 0.999)$	(19)
Projecting (exposed invert)	$\Delta r/D + \Delta t/D = -1.008\ (r_e/D)^2 + 6.403 \times 10^{-1}\ (r_e/D) + 6.678 \times 10^{-2} \mid (R^2 = 0.997)$	(20)

Table 9. Elliptical arc geometry – derived using eq. 6 and 7.

$\theta_t = 10.0^\circ$			$\theta_t = 20.0^\circ$			$\theta_t = 33.7^\circ$		
η [°]	x/D [-]	z/D [-]	η [°]	x/D [-]	z/D [-]	η [°]	x/D [-]	z/D [-]
10.0	0.000	0.000						
15.0	0.047	0.008						
20.0	0.082	0.018	20.0	0.000	0.000			
25.0	0.109	0.028	25.0	0.021	0.008			
30.0	0.132	0.038	30.0	0.039	0.016	33.7	0.000	0.000
35.0	0.151	0.049	35.0	0.054	0.025	37.0	0.008	0.005
40.0	0.167	0.060	40.0	0.067	0.034	40.0	0.015	0.010
45.0	0.181	0.072	45.0	0.078	0.043	45.0	0.025	0.019
50.0	0.193	0.084	50.0	0.087	0.052	50.0	0.033	0.027
55.0	0.202	0.095	55.0	0.095	0.061	55.0	0.040	0.036
60.0	0.210	0.106	60.0	0.101	0.070	60.0	0.046	0.044
65.0	0.215	0.116	65.0	0.106	0.078	65.0	0.051	0.052
70.0	0.220	0.125	70.0	0.109	0.085	70.0	0.054	0.059
75.0	0.222	0.132	75.0	0.111	0.091	75.0	0.056	0.064
80.0	0.224	0.138	80.0	0.112	0.096	80.0	0.057	0.069
85.0	0.224	0.142	85.0	0.113	0.099	85.0	0.058	0.072
90.0	0.225	0.143	90.0	0.113	0.100	90.0	0.058	0.073
180.0	0.225	0.200	180.0	0.113	0.184	180.0	0.058	0.153